High Temperature Resin/ Carbon Nanotube Composite Fabrication

Sayata Ghose,[1] Kent A. Watson,[2] Keun J. Sun,[2] Jim M. Criss,[4] Emilie J. Siochi,[3]

John W. Connell[3]*

[1]National Research Council

[2] National Institute of Aerospace

100 Exploration Way, Hampton, VA 23666

[3]NASA Langley Research Center

Hampton, VA 23681-2199

[4]M & P Technologies, Inc.

Marietta, GA 30068

Abstract

For the purpose of incorporating multifunctionality into advanced composites, blends of PETI-330 and multi-walled carbon nanotubes (MWCNTs) were prepared, characterized and fabricated into moldings. PETI-330/MWCNT mixtures were prepared at concentrations ranging from 3 to 25 weight percent by dry mixing the components in a ball mill. The resulting powders were characterized for degree of mixing, thermal and rheological properties. Based on the characterization results, PETI-330/MWCNT samples were scaled up to ~300 g and used to fabricate moldings by injecting the mixtures at 260-280 °C into a stainless steel tool followed by curing for 1 h at 371 °C. The tool was designed to impart a degree of shear during the injection process in an attempt to achieve some alignment of the

MWCNTs in the flow direction. Obtained moldings were subsequently characterized for thermal, mechanical, and electrical properties. The degree of dispersion and alignment of MWCNTs were investigated using high-resolution scanning electron microscopy. The preparation and preliminary characterization of PETI-330/MWCNT composites will be discussed.

* To whom correspondence should be addressed: john.w.connell@nasa.gov, (757) 864-4264

INTRODUCTION

Thermally stable, high-performance resins are required for use in composite structures on aerospace vehicles such as supersonic aircraft and reusable launch vehicles. Due to an excellent combination of physical and mechanical properties, aromatic polyimides are leading candidates for these applications [1, 2]. However, polyimides are difficult to fabricate into composites and in an attempt to improve their processability, controlled molecular weight imide oligomers containing phenylethynyl groups have been developed. Phenylethynyl groups are thermally unreactive up to 300 °C, but react rapidly at temperatures of 350-371 °C without volatile evolution to yield a cross-linked resin [3 - 14]. The combination of a large processing window and the formation of a product exhibiting good toughness, good microcrack resistance, and excellent thermo-oxidative stability makes phenylethynyl terminated imide (PETI) technology very attractive for use in high performance composite and adhesive applications. PETI-330 is a low molecular weight imide oligomer that has a low and stable melt viscosity at 280 °C and a glass transition temperature of 330 °C after curing at 371 °C. PETI-330 has been used for making composites by resin transfer molding (RTM), vacuum-assisted RTM (VARTM), and resin infusion (RI) and the laminates exhibit excellent properties [9,10].

Material needs on some advanced aerospace vehicles such as Gossamer spacecraft require multifunctional capabilities. For example, the incorporation of carbon nanotubes (CNTs) into aromatic polyimide films provides sufficient electrical

conductivity to dissipate electrostatic charge (ESC) build up without degrading mechanical properties or flexibility or significantly compromising the thermo-optical properties [15]. When CNTs are thoroughly dispersed in the polymeric material, an interconnecting network of CNTs is formed which provides a pathway for electrical charge to flow. Various methods have been attempted for achieving good dispersion of CNTs in the polymer. They include the preparation of the polymer in the presence of CNTs under sonication [16] and the use of alkoxysilane terminated amide acid oligomer to disperse the CNTs [17]. In applications where only surface conductivity is required, single-walled carbon nanotubes (SWCNTs) were spray-coated on the surface of the polymer substrates [15]. In all these experiments, CNT concentration was minimized in order to retain the optical properties of the films.

Unlike thin films needed for Gossamer spacecraft, structural components do not require optical transparency or low color [18]. Thus the incorporation of multi-walled carbon nanotubes (MWCNTs), which are less expensive and have a lower aspect ratio relative to SWCNTs, was investigated as a means to impart both structural and electrical properties. The goal of this research was to incorporate a sufficient concentration of MWCNTs to affect electrical conductivity and modulus improvement without severely reducing the melt flow properties (i.e., processability) of the matrix resin. The approach taken involves a dry mixing technique for incorporating MWCNTs. Maintaining melt flow properties is important because melt processing is generally the preferred method of fabricating composites from PETI-330. However this process has not been extensively used for nanocomposites

because CNTs tend to agglomerate under these conditions and at high loading levels the viscosity becomes too high for processing. Usually, this can be minimized by the appropriate application of shear during mixing. For example, polymethylmethacrylate (PMMA) containing SWCNTs has been produced using a combined method of solvent casting and melt mixing [19]. A miniature mixer-molder has also been used to produce small quantities of well-dispersed mixtures of MWCNTs in PMMA [20]. The mixtures were then compressed into thin films and measurements of their dynamic mechanical behavior showed an increase in storage modulus.

Another recent method to disperse MWCNTs uses a micro-scale twin-screw extruder. This device has been used for the melt mixing of MWCNTs with polycarbonates [21] and polystyrene [22]. The high shear mixing necessary to disentangle and uniformly disperse MWCNTs in the matrix can be achieved with the extruder. The process of extruding nanocomposite through a suitable die and subsequent drawing yields continuous ribbons of nanocomposites with aligned nanotubes that can be further processed into laminates having improved elastic modulus and yield strength compared to randomly oriented nanocomposites [22]. Morphological studies using transmission electron microscopy (TEM) and scanning electron microscopy (SEM) have shown interconnecting structures formed by the nanotubes that efficiently help in load transfer between the polymer matrix and nanotube reinforcement [21, 22]. SWCNTs have been incorporated (up to 1 % by weight) into Ultem™ 1000, a thermoplastic polyetherimide, and melt processed to

yield fibers [23]. Although the melt process was not optimized to fully disperse and align the SWCNTs, some improvements in mechanical properties were achieved. Typically melt processing works better for thermoplastics than thermosets due to melt stability in the required processing window. However, oligomers endcapped with reactive phenylethynyl groups possess the appropriate combination of processing characteristics for melt processes like injection molding or extrusion.

Ball-milling is a mechanical process that leads to local generation of high pressure as a result of collisions throughout the grinding media [24]. This method has been used to obtain nano-barrels from cup-stacked carbon nanotubes [25], transform nanotubes into nanoparticles (ellipsoidal and spherical) [26], generate nanostructures from graphite [27 - 28], and shorten the lengths of nanotubes [29 - 30]. Polyethylene terephthalate (PET) was compounded with various grades (5 wt %) of carbon nanofibers (CNF) by ball-milling [31] followed by extrusion or melt mixing. The impact of ball-milling on MWCNTs has been studied [32, 33] but to date there is no reported work on dry compounding of polymers with MWCNTs using the ball mill.

The successful fabrication of nanocomposites that contain high loadings (>3 wt %) of CNTs has been elusive. The objective of this research was to combine PETI-330 with high loadings of MWCNTs using a dry mixing technique like ball-milling prior to fabricating nanocomposites by injection molding. Preparation of samples containing various loading levels of MWCNTs followed by their characterization has already been studied [34]. Based on viscosity and processing

properties, samples were chosen for injection molding and the molded plaques were subsequently characterized.

EXPERIMENTAL

Materials

PETI-330 was obtained from JFC Technologies, Bound Brook, NJ and the MWNTs (35 – 50 nm diameter according to manufacturer) were procured from The University of Kentucky, Lexington, KY and used as received.

Preparation of PETI-330 with various % (wt/wt) MWCNT: dry mixing

Dry mixing of PETI-330 and MWCNTs was carried out in alumina-fortified porcelain jars using cylindrically shaped zirconia grinding media (9.5 mm x 9.5 mm). The jars were placed on rollers and rotated for 48 h at 120 rpm. After mixing, the grinding media was separated from the powder using a sieve and the powder was collected. Typical recovery yields ranged from 80 to 90 % of the total weight due to some adhesion of powder to the jar and grinding media.

Composite Specimens of PETI-330/MWCNT

An Invar® tool designed such that the injection ports are tapered to provide shear during injection to induce some orientation of the MWCNTs was used in the molding fabrication. Approximately 300 g of PETI-330/MWCNT sample was degassed in the injector by heating to 280 °C and holding for 1 h prior to injection. The high temperature injector was built by Radius Engineering according to

Lockheed Martin specifications and can operate at a maximum temperature of 288 °C, flow rate of 500 cc/min, and pressure of 2.75 MPa. The degassing step is generally required in RTM primarily to remove moisture and air from the material. After the resin was injected at 288 °C at a rate of 200 cc/min, the tool was held in a press at a minimum of 1.38 MPa of hydrostatic pressure in order to assure adequate sealing, heated to 371 °C and held at this temperature for 1 h. The plaques were cooled in the mold.

Characterization

Dynamic rheological measurements were obtained using an Advanced Rheometric Expansion System (ARES) from Rheometrics, Inc. Measurements were carried out under nitrogen in an oscillatory shear mode using parallel plate geometry (30 mm diameter). Discs of the samples were prepared by compression molding approximately 0.75 g of sample at room temperature and subsequently inserting this into the test chamber at 100 °C. The top plate was oscillated at a variable strain and a fixed angular frequency of 100 rad/s while the lower plate was attached to a transducer that recorded the resultant torque. Specimens were heated to 280 °C at a rate of 4 °C/min and held at 280 °C for 2 h to assess melt stability. Heating was then continued at the same rate to 371 °C and held for 100 s. High-resolution scanning electron microscope (HRSEM) images were obtained using a Hitachi S-5200 field emission scanning electron microscope (FE-SEM) equipped with a "through-the-lens" secondary electron detector operating at or below 1 kV.

Composite images were obtained in low voltage mode in order to set up a stable local electric field on the sample while minimizing beam-induced damage. Both the powder and the sample obtained from the ARES were scanned.

Thermal conductivity of the plaques was measured using a Netzsch LFA 447 NanoFlash according to ASTM E1461. Samples (1 cm x 1 cm) were coated with a thin layer of graphite (for uniform thermal adsorption), which was rinsed away with solvent (e.g. methanol). Pyrex (TC ~ 1.09 W/mK, Cp ~ 0.76 J/gk) was used as the reference. Surface and volume resistivities of the plaques were measured using a Prostat® PRS-801 Resistance System with a PRF-911 Concentric Ring Fixture operating per ASTM D-257 and reported as an average of three readings. Measurements were taken before and after the plaques were polished using a Ecomet-4 Variable Speed Grinder-Polisher. A load of 9.07 kg-force and sanding grits of 60 and 100 were used for polishing each plaque. Surface resistance was also measured using a Kethley Sub-Femtoamp Remote Source Meter (Model 6430). Samples were mounted on a Summit 11000/12000 B-Series Probe Station (Cascade Microtech). Distance between the two probes was 0.18 cm with a current of 1 µA applied to each sample. Hardness tests were performed on the molded plaques using a Wilson Rockwell Hardness Tester (Series 2000). A 1.5875 mm diameter hardened steel ball was used for Test HRT15 with an initial load of 3 kg and a total load of 15 kg. Hardness of the neat resin and composite plaques was also measured using a Shore D durometer according to ASTM D2240 with the plaques being treated as hard plastics. Tensile properties were evaluated using a Sintech 2W load

frame and Testworks 4 software with a load cell of 1.334 kN (300 lb-force), crosshead speed of 5.08 mm/min and gauge length of 22 mm. Samples were prepared according to ASTM D1708 and machined using a Bengal 20 x 40 Water Jet (Flow Corporation).

RESULTS AND DISCUSSION

Characterization of Nanocomposite Powder:

1. Melt viscosity of ball-milled PETI-330/ MWCNT samples

The complex viscosity of the neat as well as MWCNT-loaded PETI-330 samples was determined from rheology using the ARES. Figure 1 shows the melt viscosity curves of neat and MWCNT loaded samples. The melt viscosity of the samples at 280 °C is important as the resin is typically injected at this temperature. The neat resin has a low melt viscosity between 5 and 10 poise (P). At 280 °C and a fixed strain rate, the viscosity values show an increasing slope with time. The phenylethynyl groups do not readily react at this temperature so no significant curing of the resin occurs. PETI-330 was independently tested in the DSC and no reaction was observed on samples held at 280 °C for 2 h. As anticipated, when heating was resumed after 2 h, viscosity showed a decrease with increasing temperature. When the temperature reached >300 °C, the phenylethynyl group started to react and consequently the viscosity increased. For the MWCNT-filled samples, melt viscosity was reasonably steady at 280 °C and increased with higher MWCNT loading.

2. HRSEM of Ball-milled and ARES Samples

HRSEM was carried out on both the powdered samples obtained from ball milling as well as samples obtained after rheometery. As shown in Figure 2, at lower magnifications the nanotubes seem to be well dispersed in the polymer matrix, more so in the 20 wt % sample. At higher magnifications, individual nanotubes can be discerned and the tubes do not seem to be damaged as a result of ball-milling or rheology experiments. HRSEM images of the powders from ball milling (Figure 3), show an abundance of MWCNTs between polymer particles especially at higher loading levels.

Characterization of Nanocomposite Plaques:

 PETI-330/MWCNT moldings, 10.2 cm x 15.2 cm x 0.32 cm and containing 10 and 15 wt% MWCNT, were prepared by injecting the samples into a specially designed tool (Figure 4) and curing at 371 °C for 1 h. Even though the 20 wt % sample had a melt viscosity of ~6000 P, it jammed the injector and no plaques could be produced. Evidently the viscosity was higher than the tolerable melt viscosity suitable for molding the plaques.

1. HRSEM on Nanocomposite Plaques

When examined by HRSEM, no tubes were observed on the surface of the moldings for the 10 wt % sample. However, the sample did not burn indicating sufficient electrical conductivity suggesting that the tubes are probably well

dispersed below the surface. As seen in Figure 5(a), the outline of the tubes can be seen beneath the surface and they appear to be aligned in the direction of resin flow in the mold as indicated by the arrow. When the fractured edge was examined, as seen in Figure 5(b), an abundance of MWCNTs was observed. When the surface of the 15 wt % sample was examined again after it had been polished, many nanotubes are visible (Figure 5c). For the 15 wt % sample, the fractured edge of test specimen (Figure 5d) for mechanical testing was also examined to reveal well dispersed MWCNTs.

2. Hardness

Hardness is defined as the property of a material that enables it to resist plastic deformation, usually by penetration. Hardness testing of plastics is most commonly measured by the Rockwell hardness test or Shore (Durometer) hardness test and these methods measure the resistance of the plastic toward indentation [35]. Both scales provide an empirical hardness value that doesn't correlate to other properties or fundamental characteristics. Rockwell hardness is generally chosen for 'harder' plastics such as nylon, polycarbonate, polystyrene, and acetal where the resiliency or creep of the polymer is less likely to affect the results. Data from this test is a useful measure of relative resistance to indentation of various grades of plastics. However, the Rockwell hardness test does not serve well as a predictor of other properties such as strength or resistance to scratches, abrasion, or wear. Both Rockwell and Shore D hardness of the plaques were determined and the values are

given in Table 1. HR, the Rockwell hardness number of a material, is given by the equation

$$HR = E - e$$

where E is a constant of 100 units for diamond and ball indenters and e is the permanent increase in depth of penetration due to major load, measured in units of 0.001 mm. In this case, MWCNT-filled samples showed a lower hardness value compared to the neat resin. A lower HR value indicates a greater depth of effective penetration or an enhanced plastic deformation of the material.

3. Electrical Properties

Surface and volume resistivities of the plaques were measured as per ASTM D-257 using Prostat® PRS-801 Resistance System (units: Ω/sq) (see Table 2). Polishing the plaques served to decrease the surface resistivity. The plaque of neat resin was electrically insulating and the resistivity decreased with an increase in the concentration of MWCNTs. Typically for electrostatic charge dissipation to occur, the surface resistivity should be between 10^6 and 10^{10} Ω/sq [36]. With the addition of MWCNTs, the plaques are now in the conductive range. Another type of surface resistivity (units: Ω/cm) was measured by a two-point probe system. Here, too, the neat samples did not show any conductivity whereas the MWCNT-filled samples were in the conductive range.

4. Thermal Conductivity

Thermal conductivity was measured using Nanoflash and following ASTM E-1461. The instrument allows a direct measurement of thermal diffusivity (α) and a comparative measurement of heat capacity (Cp). The thermal conductivity (λ), is calculated as $\lambda = \alpha \, \rho \, Cp$. Table 3 shows the thermal conductivity data of neat and MWNT-filled samples. With a loading of 10 wt %, conductivity was improved ~3-fold while with 15 wt % loading the improvement is close to 4 times. This suggests that nanotubes are forming an effective network in the polymer matrix which conducts heat.

5. Mechanical Properties

Tensile properties of PETI-330/MWCNT samples were evaluated. Investigations on the physical appearance of samples were carried out using optical microscopy (Olympus BH-2) at a magnification of 5x. Figure 6 shows voids that are representative of most samples. During tensile testing the voids act as defect sites that initiate premature mechanical failure, resulting in lower mechanical properties and rendering the data unusable. The source of the voids is unclear but they may be due to volatilization of low molecular weight oligomers within the matrix. PETI-330 was developed as a composite matrix resin where void formation from oligomer volatilization was not an issue in the composite processing.

SUMMARY

The fabrication of polyimide nanocomposites containing up to 15 wt % MWCNTs was possible without exceeding the maximum tolerable melt viscosity for composite processing. Select samples were scaled up for processing and plaques were prepared by injecting samples into a specially designed tool followed by curing. Hardness measurements indicate enhanced plastic deformation in the samples. The neat resin proved to be insulative but the plaques were conductive with surface resistivity values of 10^3 - 10^4 Ω/sq. Incorporation of MWCNTs also improved the thermal conductivity of PETI-330 samples. However, molded samples contained voids and mechanical properties were inconclusive due to these defects. Further efforts are necessary to develop void-free samples that should give more accurate mechanical data.

Acknowledgement
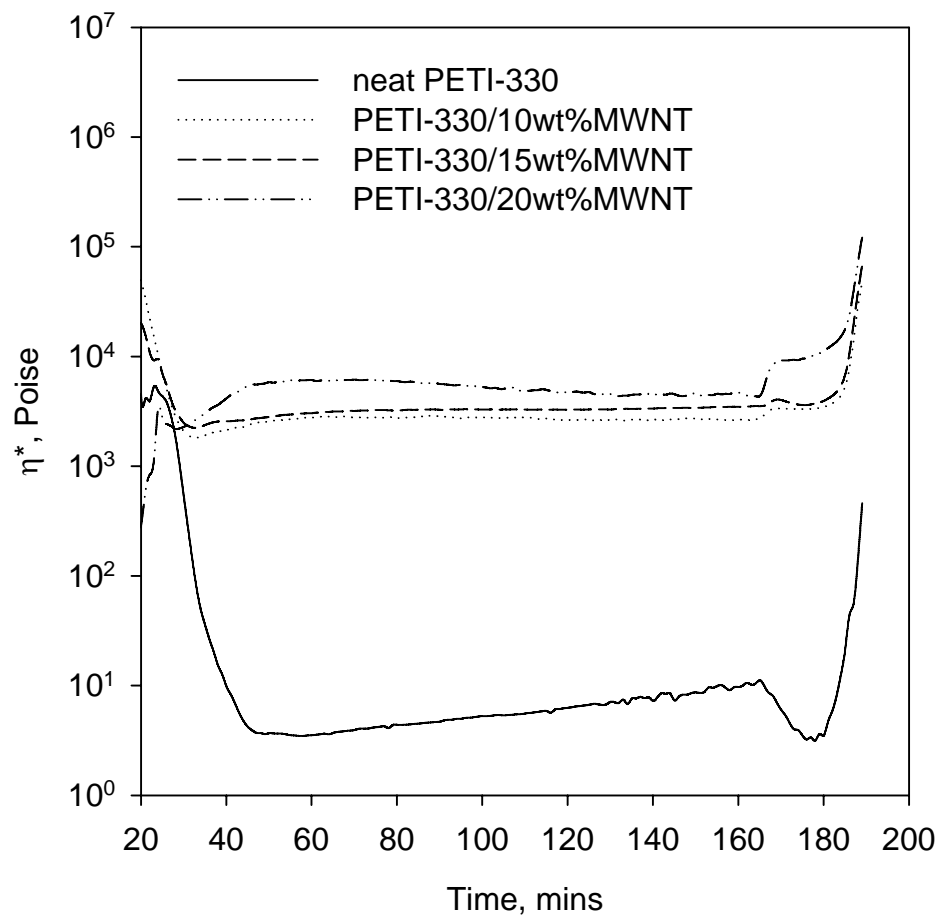
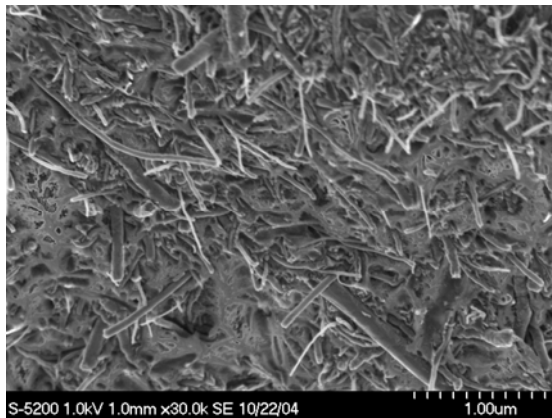Figure 1: Complex melt viscosity of PETI-330 with various amounts of MWCNTs
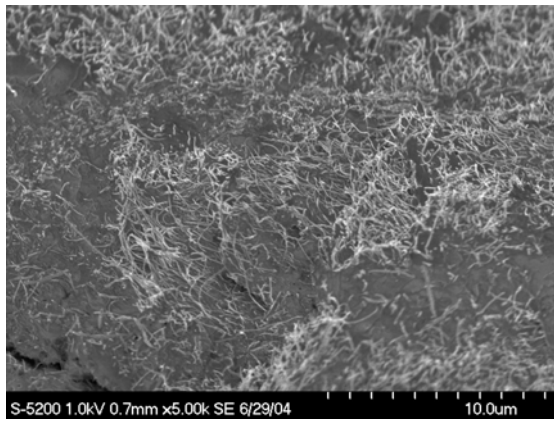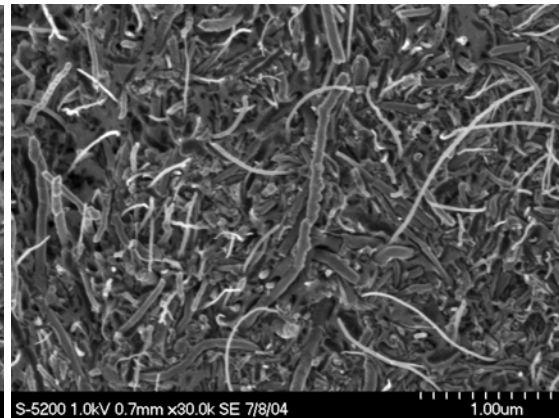
(a) 10 wt % MWCNT
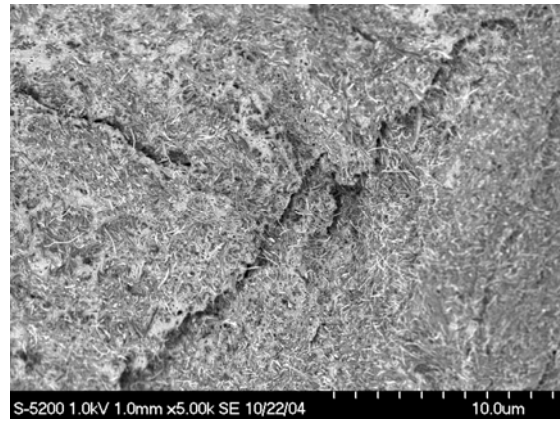
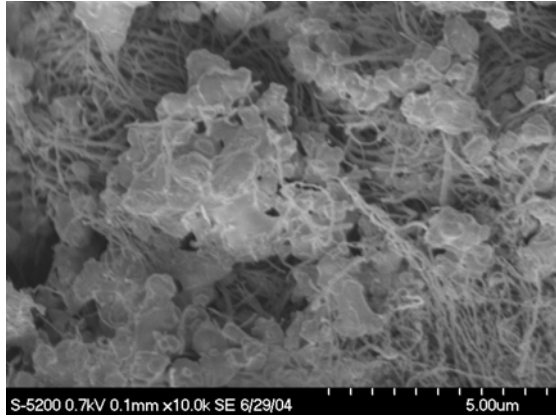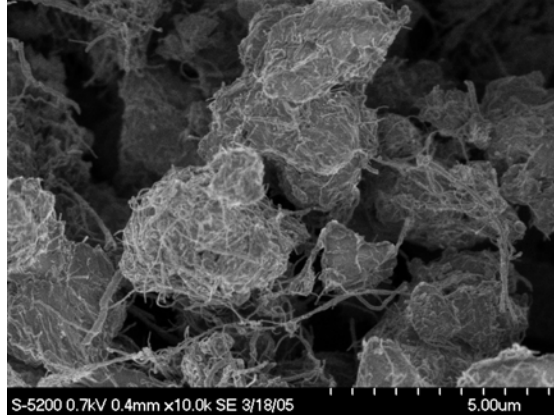(b) 15 wt % MWCNT
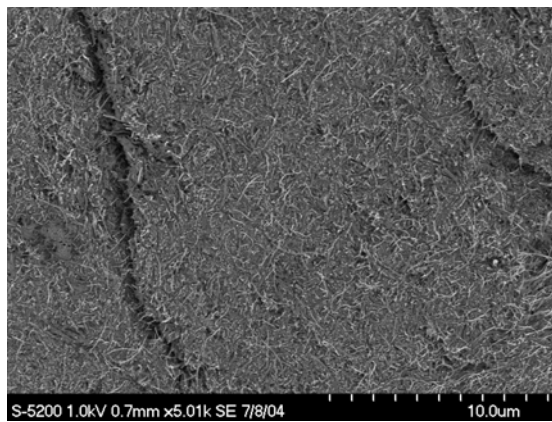
(c) 20 wt % MWCNT
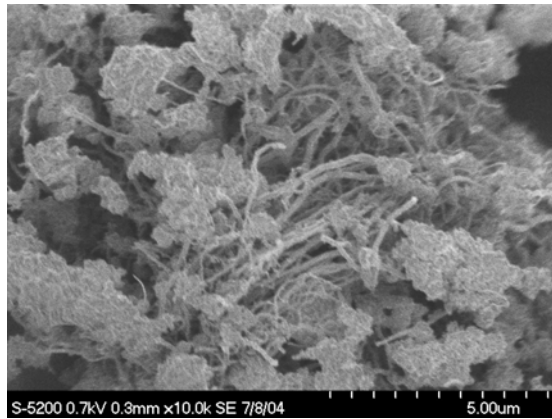

(d) 15 wt % MWCNT

(e) 20 wt % MWCNT

Figure 2: HRSEM of MWCNT-filled PETI-330 samples as obtained from the ARES; (d) and (e) are at higher magnifications.
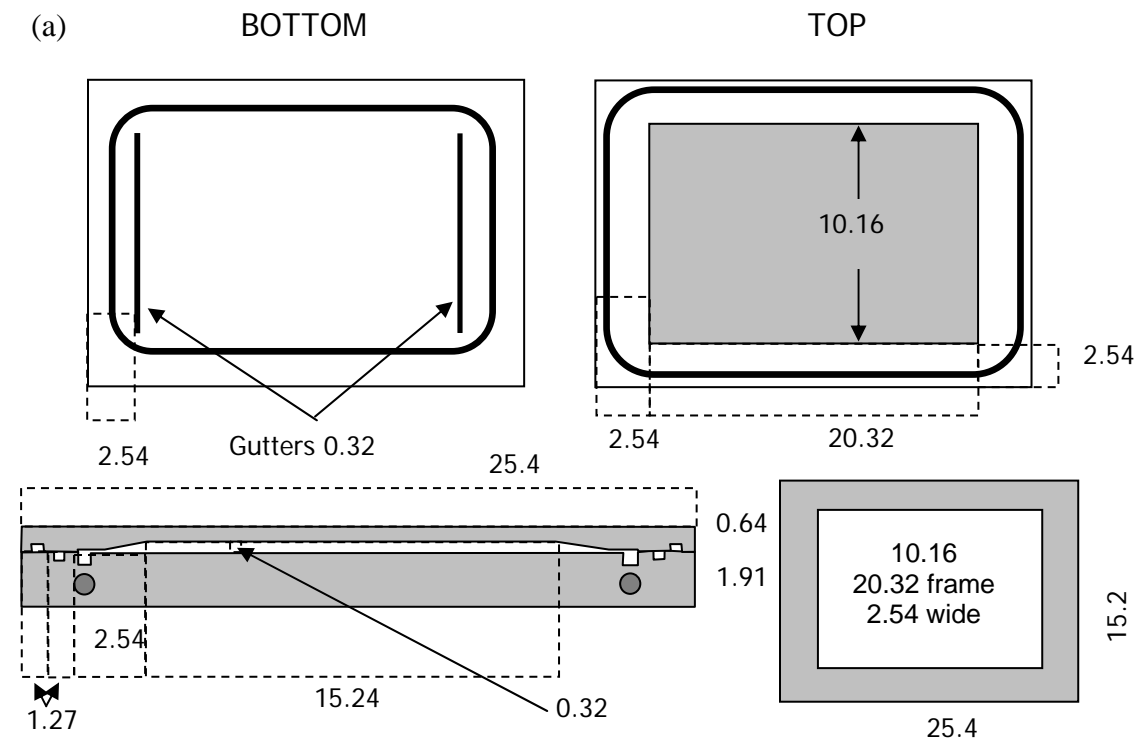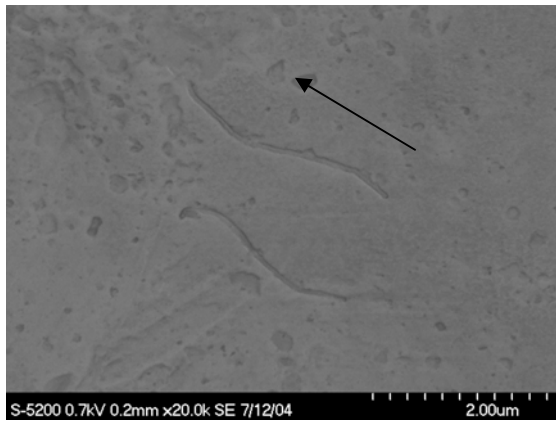
10 wt % MWCNT

15 wt % MWCNT

20 wt % MWCNT

Figure 3: HRSEM of MWCNT-filled PETI-330 samples as obtained from ball-milling

(a) BOTTOM   TOP

10.16

2.54

2.54   20.32

Gutters 0.32

2.54

25.4

0.64

1.91

10.16
20.32 frame
2.54 wide
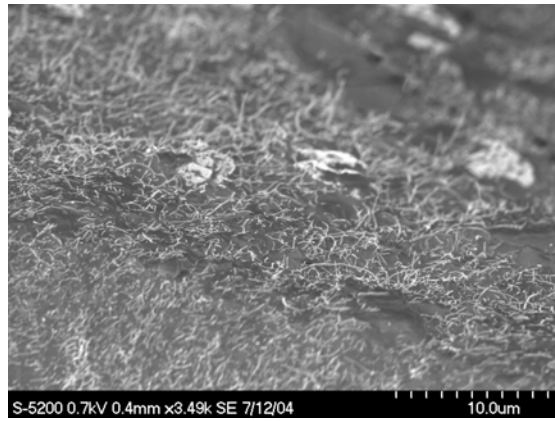
15.2

2.54

15.24

1.27

0.32

25.4

(b)

Figure 4: Tool for injection molding of PETI-330/MWNT plaques; a) schematic (all dimensions in cm) b) photograph
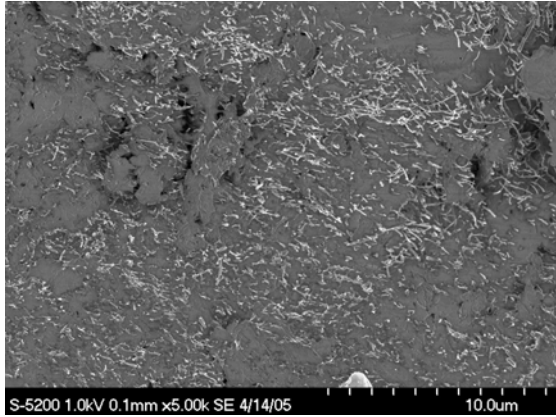
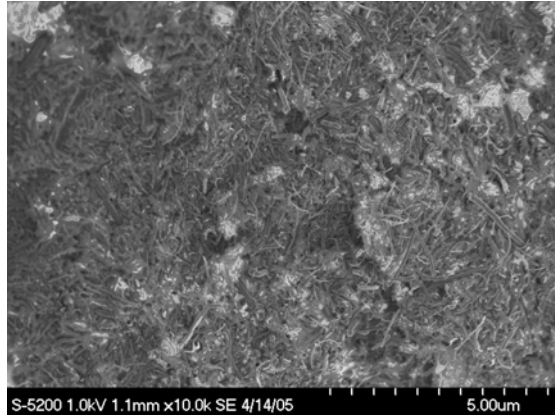(a) Top surface (before polishing)   (b) Fractured surface
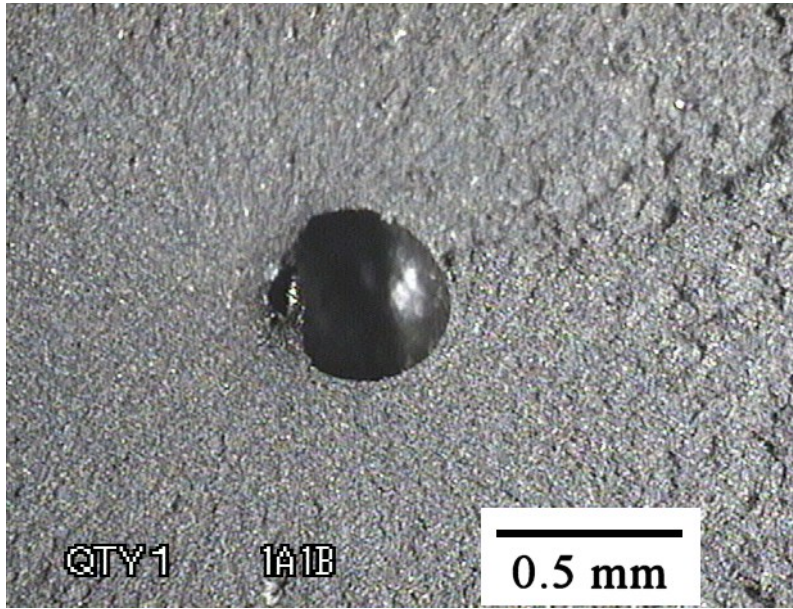
10 wt % MWCNT sample

(c) Top surface (after polishing)   (d) Fractured surface from mechanical
testing

15 wt % MWCNT sample

Figure 5: HRSEM of injection-molded plaques of MWCNT-filled PETI-330

Fractured surface of PETI-330/15 wt % MWCNT

Top surface of PETI-330/10 wt % MWCNT

Figure 6: Optical microscope pictures of sample defects

Table 1: Hardness of PETI-330/MWCNT plaques:

Sample	Shore D hardness	Rockwell hardness	
		Top surface	Bottom surface
Neat	89	84.4	84.7
10 wt % MWCNT	88	79.7	79.3
15 wt % MWCNT	89	78.9	79.1

Table 2: Electrical properties of PETI-330/MWCNT plaques:

Sample	Surface resistivity, Ω/cm	Surface resistivity		Volume resistivity, Ω-cm
		Top Ω/sq	Bottom, Ω/sq	
Neat	insulative	$> 10^{12}$	$> 10^{12}$	insulative
10 wt % MWCNT	8.9×10^3	1.8×10^4	1.9×10^4	5.5×10^4
15 wt % MWCNT	5.1×10^3	8.7×10^3	1.6×10^4	2.3×10^4

Table 3: Thermal conductivity of PETI-330/MWCNT plaques:

Sample	Thickness, mm	Specific gravity	Cp, J/gK	Diffusivity, mm^2/s	TC (W/mK)
Neat	2.417	1.305	1.199	0.140	0.219
10 wt % MWCNT	2.769	1.333	1.237	0.350	0.577
15 wt % MWCNT	2.697	1.367	1.309	0.434	0.777

References

1. Wilson D, Stenzenberger HD, Hergenrother PM. "Polyimides", Blackie and Sons Ltd., Glasgow, UK, (1990).

2. Hergenrother PM. High Performance Polymers, 2003; 15 (1): 3.

3. Connell JW, Smith Jr JG, Hergenrother PM, Rommel ML. Intl. SAMPE Tech. Conf. Series 1998; 30: 545.

4. Criss JM, Connell JW, Smith Jr. JG. Intl. SAMPE Tech. Conf. Series 1998; 30: 341.

5. Criss JM, Arendt CP, Connell JW, Smith Jr. JG, Hergenrother PM. SAMPE J 2000; 36 (3): 32.

6. Smith Jr. JG, Connell JW, Hergenrother PM, Criss JM. Soc. Adv. Mat. Proc. Eng. Ser. 2001; 46: 510.

7. Smith Jr. JG, Connell JW, Hergenrother PM, Criss JM. J. Comp. Matls 2002; 36 (19): 2255.

8. Criss JM, Koon RW, Hergenrother PM, Connell JW, Smith Jr. JG. Intl. SAMPE Tech. Conf. Series 2001; 33: 1009.

9. Smith Jr. JG, Connell JW, Hergenrother PM, Yokota R, Criss JM. Soc. Adv. Mat. Proc. Eng. Ser. 2002; 47: 316.

10. Smith Jr. JG, Connell JW, Hergenrother PM, Ford LA, Criss JM. Macromol. Symp. 2003; 199: 401.

11. Connell JW, Smith Jr. JG, Hergenrother PM, U.S. Patent 6,359,107 B1 to NASA (2002).

12. Criss JM, Meador MA, Chuang KC, Connell JW, Smith Jr. JG, Hergenrother PM, Mintz EA, Soc. Adv. Mat. Proc. Eng. Ser. 2003; 48: 1063.

13. Connell JW, Smith Jr. JG, Hergenrother PM, Criss JM. Intl. SAMPE Tech. Conf. Series 2003; 35.

14. Connell JW, Smith Jr. JG, Hergenrother PM, Criss JM, Soc. Adv. Mat. Proc. Eng. Ser.2003; 48: 1076.

15. Watson KA, Ghose S, Delozier DM, Smith Jr. JG, Connell JW, Polymer 2005; 46: 2076.

16. Park C, Ounaies Z, Watson KA, Crooks RE, Smith Jr. JG, Lowther SE, Connell JW, Siochi EJ, Harrison JS, St. Clair, TL. Chem. Phys. Lett. 2002; 364: 303.

17. Smith Jr. JG, Connell JW, Hergenrother PM. 46th International SAMPE Symposium and Exhibition 2001; 46: 510.

18. Connell JW, Watson KA. in Gossamer Spacecraft: Membrane and Inflatable Structures Technology for Space Applications, Vol. 191 p 243, C.H.M. Jenkins Ed., American Institute of Aeronautics and Astronautics, Inc., Reston, VA, USA

19. Haggenmueller R, Gommans HH, Rinzler AG, Fischer JE, Winey KI. Chem Phys Lett 2000; 330: 219.

20. Jin Z, Pramoda KP, Xu G, Goh SH. Chem Phys Lett 2001; 337: 43.

21. Potschke P, Fornes TD, Paul DR. Polymer 2002; 43: 3247.

22. Thostenson ET, Chou T. J. Phys. D: Appl. Phys. 2002; 35: L77.

23. Siochi EJ, Working DC, Park C, Lillehei PT, Rouse JH, Topping CT, Bhattacharya AR, Kumar S. Composites: Part B 2004; 35: 439.

24. Konya Z, Zhu J, Niesz K, Mehn D, Kiricsi I. Carbon 2004; 42: 2001.

25. Kim YA, Hayashi T, Fukai Y, Endo M, Yanagisawa T, Dresselhaus M. Chem. Phys. Lett. 2002; 355 (3-4): 279.

26. Li YB, Wei BQ, Liang J, Yu Q, Wu DH. Carbon 1991; 37: 493.

27. Awasthi K, Kamalakaran R, Singh AK, Srivastava ON. Int J Hydrogen Energy 2002; 27: 425.

28. Huang JY, Yasuda H, Mori H. Chem. Phys. Lett. 1999; 303 (1-2): 130.

29. Pierard N, Fonseca A, Konya Z, Willems I, van Tendeloo G, Nagy JB. Chem. Phys. Lett. 2001; 335 (1-2): 1.

30. Pierard N, Fonseca A, Colomer JF, Bossuot C, Benoit JM, van Tendeloo G, Nagy JB. Carbon 2004; 42: 1691.

31. Kumar S, Uchida T, Dang T, Zhang X, Park Y. Soc. Adv. Mat. Proc. Eng. Ser.2004; 49.

32. Kukovecz A, Kanyo T, Konya Z, Kiricsi I, Carbon 2005; 43: 994.

33. Tao Z, Geng H, Yu K, Yang Z, Wang Y. Materials Letters 2004; 58 (27-28): 3410.

34. Ghose S, Watson KA, Delozier DM, Working DC, Siochi EJ, Connell JW. Composites Part A (in press).

35 http://www.calce.umd.edu/general/Facilities/Hardness_ad_.htm

36. Smith Jr. JG, Watson KA, Connell JW, Delozier DM, Lillehei PT, Lin Y, Zhou B, Sun YP. Polymer 2004; 45: 825.